International Journal of Sediment Research 39 (2024) 464–477

Contents lists available at ScienceDirect

International Journal of Sediment Research

journal homepage: www.elsevier.com/locate/ijsrc

Original Research

Post-fire erosion and sediment yield in a Mediterranean forest catchment in Italy

Giovanni Mastrolonardo [a], Giulio Castelli [a, b, c, *], Giacomo Certini [a], Melanie Maxwald [a, d], Paolo Trucchi [a], Cristiano Foderi [a], Alessandro Errico [a], Elena Marra [a, f], Federico Preti [a, e]

[a] Dipartimento di Scienze e Tecnologie Agrarie, Alimentari, Ambientali e Forestali (DAGRI), Università degli Studi di Firenze, Firenze, Italy
[b] UNESCO Chair in Hydropolitics, University of Geneva, Genève, Switzerland
[c] Environmental Governance and Territorial Development Hub (GEDT), University of Geneva, Genève, Switzerland
[d] Department of Civil Engineering and Natural Hazards, Institute of Soil Bioengineering and Landscape Construction (IBLB), University of Natural Resources and Life Sciences, Vienna (BOKU), Vienna, Austria
[e] Research Unit Water and Vegetation (WaVe), Università degli Studi di Firenze, Firenze, Italy
[f] Institute of Research on Terrestrial Ecosystems (IRET), National Research Council of Italy, Sesto Fiorentino (FI), Italy

ARTICLE INFO

Article history:
Received 24 April 2023
Received in revised form
10 February 2024
Accepted 26 March 2024
Available online 29 March 2024

Keywords:
Wildfire
Check dams
Post-fire hydrological modelling
Soil loss
Sediment yield
Hydrologic engineering center –hydrological modelling system (HEC-HMS)

ABSTRACT

Wildfires are an increasingly alarming phenomenon that affects forests and agroecosystems, generating several cascade effects among which soil erosion is one of the most deleterious. A robust body of data-based evidence on post-fire soil erosion and sediment yield at the watershed scale is, thus, required, especially when dealing with areas where wildfires are particularly frequent, such as the Mediterranean basin. This study analyzes the impact of the first rains after a large wildfire in terms of soil erosion and sediment yield at the watershed scale in a Mediterranean area, the Pisan Mountains, central Italy. Here about 1,000 ha of olive groves, maquis, maritime pine, and chestnut forests, all on steep slopes, burned in 2018. Fire (or burn) severity was mapped by remote sensing and checked by a field survey. Sediment yield was assessed by sampling earthy materials deposited upstream of a check dam at the outlet of the studied watershed. Finally, a hydrological model was developed in the hydrologic engineering center –hydrological modelling system (HEC–HMS) environment to explore the relationship between the erosion–deposition events observed in the watershed and the rainfall-induced hydrological processes. The first two post-fire rainy events relocated a high mass of sediment, mostly non-organic and characterized by light color, perhaps already in the stream before fire, while the subsequent four rain showers deposited materials rich in pyrogenic organic matter. Overall, the soil erosion caused by these six major rainfall events–the larger of which had a return time of one year–was estimated to amount to 7.85 t/ha (0.26 mm in the watershed), corresponding to 42% of the watershed average annual potential erosion rate in unburned conditions. This value is lower than expected, and, overall, moderate if compared to other Mediterranean case studies, possibly because of the nature of soils in the watershed, i.e., shallow and stony, thus, poor in fines prone to erosion.

1. Introduction

Post-fire soil erosion is a negative outcome of wildfires, which makes them a hydrological and geomorphological agent (Greenbaum et al., 2021; Robinne et al., 2021; Rulli & Rosso, 2007; Shakesby & Doerr, 2006; Vieira et al., 2023). Burned areas are prone to soil erosion because of decreased vegetation and litter covers, which would otherwise protect the soil against wind and water erosion (Ebel, 2020; Fernandez et al., 2016; Vega et al., 2020). Surface runoff is promoted by fire, which increases topsoil clogging and hydrophobicity, thus limiting water infiltration (Larsen et al., 2009; Rulli et al., 2006). Erosion implies a net loss of soil organic matter and soil fertility, both generally greater in the uppermost soil layers (Shakesby, 2011; Thompson et al., 1991). Furthermore, topsoil erosion reduces the potential for soils to act as carbon sinks, which is functional for mitigating climate change (Powlson et al., 2011). Last, once transported downstream the eroded soil can also cause major hydraulic problems (Robinne et al., 2021; Stavi,

* Corresponding author.
E-mail address: giulio.castelli@unifi.it (G. Castelli).

https://doi.org/10.1016/j.ijsrc.2024.03.008

2019). The eroded soil impacts surface waters with sediments and possible contaminants (Abraham et al., 2017; Granath et al., 2016), and often needs to be collected and disposed in landfills (Köthe, 2003).

Relatively few studies have been done to account for the consequences of wildfires in terms of soil erosion and sediment yield at the catchment scale compared to the plot, slope, and swale scales, perhaps because of practical and/or economic issues (Basso et al., 2019; Mayor et al., 2011; Robichaud et al., 2016; Shakesby, 2011; Weninger et al., 2019; Wu et al., 2021). However, geomorphic and hydrological processes are highly affected by the spatial scale, and, therefore, erosion rates at larger scales should not be inferred from plot-scale studies (Parsons et al., 2006). Indeed, plot- and hillslope-scale studies often overestimate hydrological and erosion processes, thus making it difficult to assess the real fire impact at a larger scale (Mayor et al., 2011; Wagenbrenner & Robichaud, 2014; Wilson et al., 2021). In a synthesis of several field studies on post-fire sediment erosion and deposition measurement across the western United States, Moody and Martin (2009) found significantly different results according to the spatial scale, although opposite to the aforementioned trend, i.e., lower sediment yield at the plot scale. In particular, they reported that the annual post-fire sediment yield measured by various authors at the catchment scale using dams, check dams, debris basins, alluvial fan deposition, and channel erosion ranged between 14 and 300 t/ha (mean 240 t/ha), while the annual sediment yield measured at hillslope scale by erosion pin, erosion bridge, survey transect, or grid measurements ranged between 37 and 160 t/ha (mean 110 t/ha) or between 6 and 200 t/ha (mean 62 t/ha), when sediment yield was measured by bounded hillslope plots, unbounded hillslope plots, and silt fences (Moody & Martin, 2009).

In the Mediterranean basin, the watershed-scale field studies on post-fire soil erosion and sediment yield are relatively fewer than in other geographic regions (Greenbaum et al., 2021; Nunes et al., 2020; Wu et al., 2021), despite some worrying aspects, such as the high frequency and severity of wildfires or the erodibility and thinness of the soils involved (Pausas et al., 2008; Poesen & Hooke, 1997). Moderate post-fire erosional events seem to prevail in the Mediterranean basin (Shakesby, 2011); however, as highlighted by Esposito et al. (2017), most of the case studies in this region are from experimental plots in Spain and Portugal. The need for larger and more representative datasets is pressing also considering that these are necessary for developing erosion models, which are more and more tested at plot and hillslope scales, but not as much at catchment or landscape scales (Basso et al., 2020; Thomas et al., 2021).

In the present study, one of the most devastating recent fires in Italy in terms of rate of spread (up to 500 m/h) and natural and structural/infrastructural damages is analyzed. It occurred in September 2018 and affected an area of about 1000 ha in the Pisan Mountains, Tuscany. The short-term impact of this fire was evaluated in terms of soil erosion and sediment yield, focusing on the first rains after the fire – usually the most problematic ones (Greenbaum et al., 2021). The study was done on a single watershed, where post-fire precipitation and the characteristics (soil organic matter content and particle size distribution) of the sediment accumulated at the catchment outlet were investigated. Substantial soil erosion and sediment yield were hypothesized because of some predisposing factors of the study area (e.g., high rainfall erosivity and steep topography). Indeed, the average annual potential erosion rate of the investigated watershed, estimated using the universal soil loss equation (USLE) method (Wischmeier & Smith, 1978) in normal conditions, is 18.8 t/ha/y (Regione Toscana, 2017), a much higher value than 4.6 t/ha/y, which is the mean erosion of the Mediterranean climatic zone (Panagos et al., 2015). The current study takes into consideration various environmental factors (e.g., burn severity, slope, soil characteristics, pre-fire land use, rainfall-runoff transformation, etc.) and makes use of a hydrological model for exploring the relationship between the erosion-deposition events and the rainfall-induced hydrological processes. This study aims to provide a contribution to the knowledge of post-fire rainfall-induced runoff processes at the catchment scale in a typical Mediterranean bio-geo-physical setting characterized by stony and shallow soils.

2. Materials and methods

2.1. Study area

The Pisan Mountains are a 15,000-ha wide ridge (maximum height 917 m a.s.l.) made of Triassic Verrucano metasediment consisting of ferriferous quartzites which have undergone relatively high-pressure and low-temperature metamorphism (Franceschelli et al., 1986; Giorgetti et al., 1998), located in central Italy, 5 km north-east of Pisa (Fig. 1). It is a fire-prone environment, having been involved in over 75 large wildfires since 1970, mainly occurring in the summertime and linked to the high anthropization of the area (Mori et al., 2023), as is usual in Mediterranean coastal areas (Pausas et al., 2008). The slope of the area ranges between 30% and 60% and the vegetation is typically Mediterranean, with olive groves and maquis in the basal belt and maritime pine or chestnut woods at higher elevations (Fig. 1). The climate is Mediterranean (Csa–"Hot-summer Mediterranean climate" in the Köppen climate classification) (Peel et al., 2007), i.e., characterized by hot and dry summers, and relatively cold and rainy falls and winters. The mean annual temperature is 14.4 °C and the mean annual precipitation is 883 mm (data source: Climate-Data.org, 2021, https//it.climate-data.org).

The current study was focused on the Santo Pietro watershed (hereafter simply called SP), which extends on the west side of the ridge (Fig. 1) and covers an area of 40.8 ha. The length of the stream is 1.12 km and the maximum, average, and outlet elevations are 409, 205, and 66 m a.s.l., respectively, corresponding to a main channel slope of 18%. The watershed is within the major Arno River basin, being located on the right side of the main river course.

According to the 1:250,000 soil map by Regione Toscana (http://sit.lamma.rete.toscana.it/websuoli/), which refers to the ninth edition of the U.S. Soil Taxonomy (Soil Survey Staff, 2003) – the soils of the area are *Ultic Haplustalfs* (fine-silty, siliceous, mesic) or *Typic Dystrustepts* (loamy-skeletal, siliceous, mesic) near the stream bed, and *Lithic Haplustepts* (loamy-skeletal, siliceous, mesic) or *Typic Dystrustepts* at higher elevations. All of these soils are historically affected by post-fire erosion. More recently, they have been involved in at least 6 relevant fires before the one of 2018 investigated here: two in 1970 (which marginally affected the upper and southern parts of SP); one in 1971, on the central part of SP; one in 1976 on over 60% of SP; one in 1989 on over 80% of SP; and one in 2011 on more than 50% of SP, mainly involving the upper part. A wooden check dam was built right after the 2018 fire at the outlet (Figs. 2 and 3), near the small town of Calci, to block the eroded soil transported by the stream, thus allowing quantification of soil erosion and reconstruction of the depositional history (see Section 2.6, Fig. 3).

2.2. Fire description and burn severity assessment

Following several relatively dry days, a fire started at 10 p.m. on September 24, 2018. Classified as a strong wind-driven crown fire with a slope-driven ground component, it burned a total area of

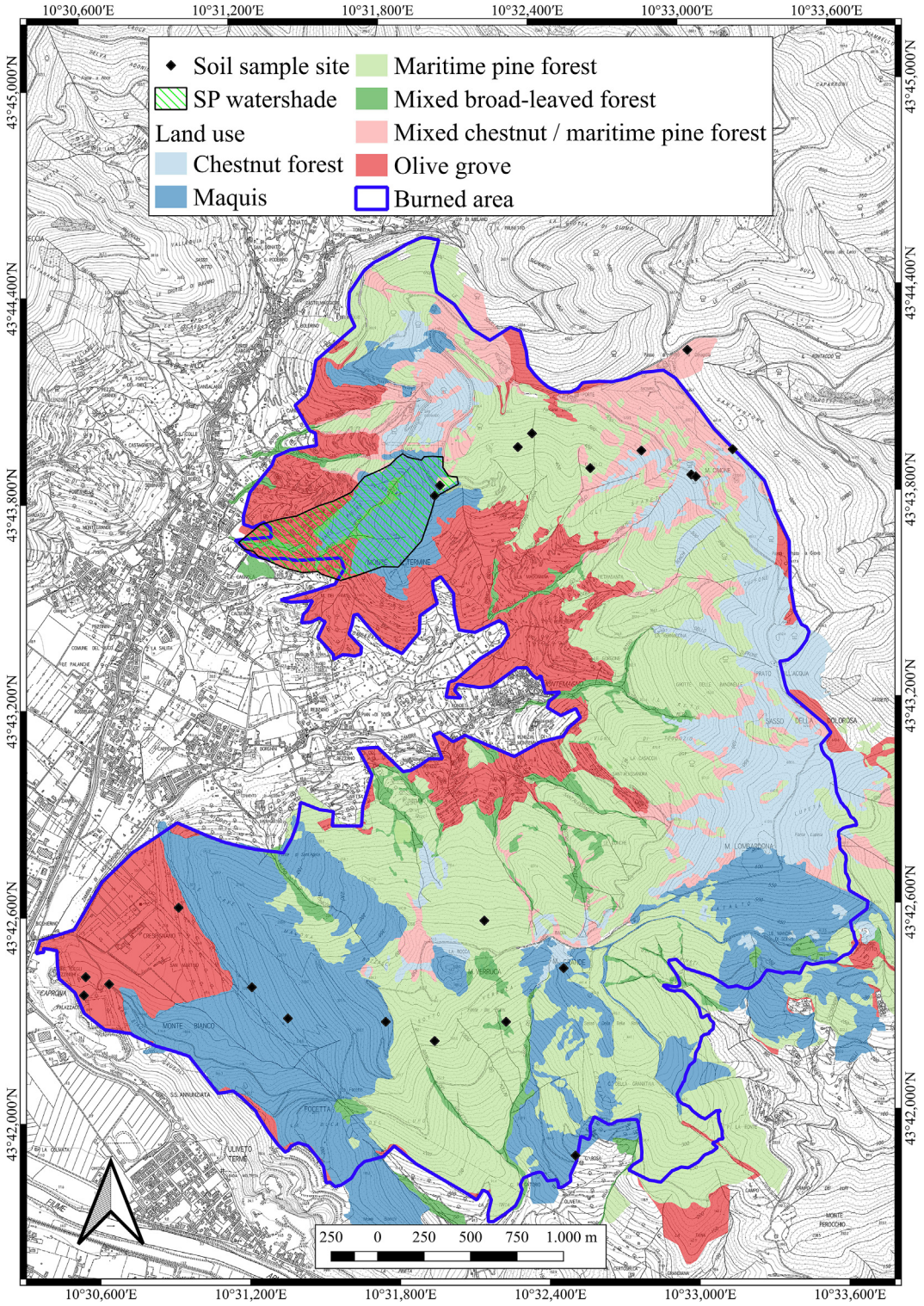

Fig. 1. Perimeter of the Pisan Mountains study area affected by the wildfire and the land uses (traced area on top). Locations of Santo Pietro (SP) watershed, check dam, and soil sampling sites are marked.

1,148 ha over three days. The wind blew with gusts of 14 m/s (50 km/h), first from north-north-east, then, in the morning of September 25 from the East. Wind speed peaks were locally measured at 22 m/s (80 km/h) by forest firefighters. A combination of slopes with wind speed and dense forest stand structure, as well as low relative humidity (40% at 9 p.m. on September 24), determined a maximum rate of spread of 500 m/h, generating several spot fires up to 8 km away from the main fire front.

The wildfire spread and intensity were dictated by the combination of several ground fires started from spot events, favored by local topography, and a main crown fire front driven by the wind. Fire control was initially restricted to property protection and

Fig. 2. Wooden check dam at the outlet of Santo Pietro watershed (photo by P. Trucchi).

perimeter containment involving 580 firefighter crews (each one composed of 2–5 operators) and 12 planes.

The assessment of burn severity was done from Sentinel-2 images (spatial resolution scaled at 20 m) recorded at the end of August and the beginning of October, calculating the relativized burnratio (RBR) index. This index indicates a relative measure of fire severity based on the difference in radiometric response between the near-infrared (NIR) and short-wave infrared (SWIR) wavelengths, measured before and after the fire (Parks et al., 2014). To improve the readability of burn severity distribution, the U.S. geological survey (USGS) classification to the RBR index (Keeley, 2009; Parks et al., 2014) (Table 1) was applied.

2.3. Field investigation and soil sampling

Fire severity was also checked by a field survey (Fig. 4), done right after the fire on the whole Pisan Mountains range area, according to the visual scale of fire severity proposed by Parsons et al. (2010). During this campaign, 20 circular areas, 30 m in diameter, five areas for each vegetation stand, i.e., maquis, pine forest, chestnut forest, and olive orchards, were selected. Sixteen of these plots were burned, and the other four were unburned (control plots), all located on the two main soil types of the area (i.e., *Typic Dystrustepts* and *Lithic Haplustepts*). In each plot, the following variables were measured in the field:

i) *Stoniness*, as the percentage presence of rock fragments >1 cm and outcrops on the surface; estimated by eye on eight circular mini-plots, with a diameter of 0.3 m, spaced 2 m from each other on an alignment.
ii) *Soil depth*, down to the bedrock, determined by a steel auger on nine randomly selected spots.

One composite soil sample was taken in each plot, bulking together three samples taken with a shovel to a depth of 1 cm (ca. 300 g each), for determining the soil texture.

2.4. Post-fire rainfall events

Our analysis was focused on the first rains after the fire. Rainfall data of interest for the current study (Fig. 5) were recorded by a station around 2.5 km from the catchment, located at an elevation of 705 m a.s.l. (Latitude 43.731°N, Longitude 10.553°E) and managed by the hydrologic regional service (SIR) of Tuscany. The first precipitation (October 28 to November 3, 2018; Fig. 5) occurred about one month after the wildfire, when five distinct intense rainy events were recorded.

The return period (R_t) of these events was analyzed by considering the specific rainfall intensity (h)–duration (t) curve in the form (Eq. (1)):

$$h = a' \cdot R_t^m \cdot t^n \tag{1}$$

where the parameters of this relation (a', m, and n) are available from the AlTo database of the Tuscany region (Preti, 2013; Preti et al., 2011). For the specific study case, they are $a' = 24.08$, $m = 0.19$, and $n = 0.31$.

2.5. Rainfall-runoff model

To explore the relationship between the erosion-deposition events monitored in the watershed and the hydrological processes induced by the rains that occurred from October 28 to November 3, 2018, a hydrological model of the SP watershed was implemented to simulate the discharge at the basin outlet. Several models have been used for simulating post-fire dynamics, including approaches based on the universal soil loss equation (USLE), modified USLE (MUSLE), and revised USLE (RUSLE) equations (e.g., Kampf et al., 2020; Zema, 2021) or eventually the soil and water assessment tool (SWAT) model (De Girolamo et al., 2022). Such simulations are on a daily timestep, or even longer, basis. An alternative is represented by process-based models (Rulli et al., 2007), which however require a detailed parametrization.

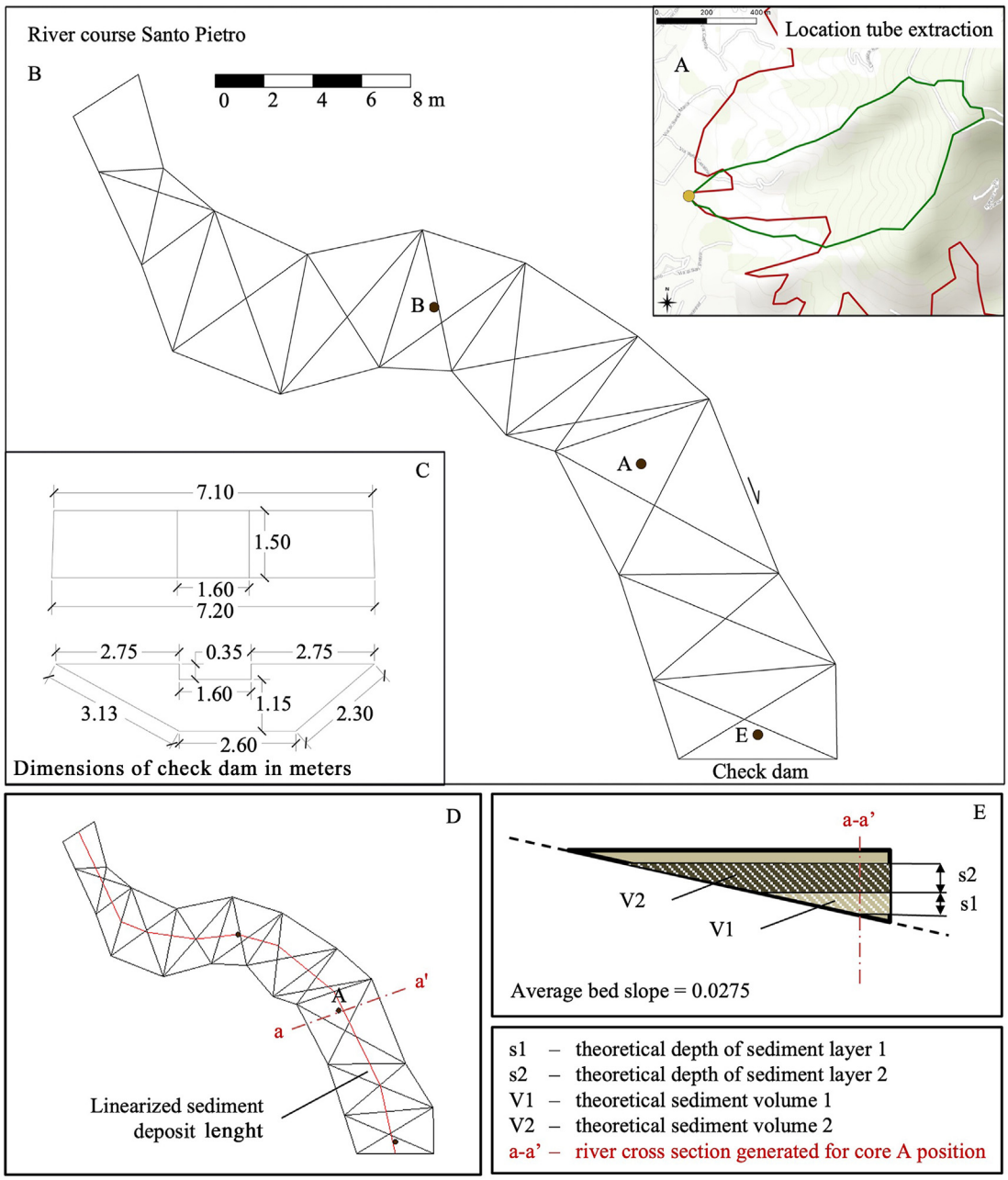

Fig. 3. (a) Location of check dam with respect to Santo Pietro watershed; (b) Locations of analyzed deposit cores and geometrical scheme for calculation of volume of sediment upstream Santo Pietro watershed check dam, and for volumes relative to each sediment layer identified in core A. (c) Check dam dimensions in meters. (d, e) Calculation schemes for deposit.

In the current study, a simplified model based on the hydrologic engineering center-hydrologic modeling system (HEC-HMS, see Scharffenberg et al., 2018) was used. HEC-HMS is a simple, globally available, and widely used software, which is a well-established standard in hydrologic simulation developed by the Hydrologic Engineering Center within the U.S. Army Corps of Engineers starting in 1992 and is still being improved. HEC-HMS was built starting from static data (land use and soil maps) and dynamics inputs (rainfall). It simulates basin-wide dynamics via sub-basins interconnected through a channel network, where rainfall-runoff generation is calculated independently for each sub-basin. The modeling of these hydrological phenomena is obtained by the simulation of the different hydrological processes, such as the rainfall partitioning between runoff, interception, and deep basin losses, the successive rainfall-runoff transformation, and the routing of river discharges in schematized flow channels. In the current study, the SP watershed was modeled with a parsimonious strategy, using a single sub-basin scheme without involving any river channel modeling, which was reasonable given the small extent of the area. Rainfall partitioning and the sub-basin loss, "loss method" section in the HEC-HMS interface, were calculated by the application of the SCS curve number (CN) method (USDA, 1986).

For each interval considered, the CN method calculates the instantaneous runoff generated (Q) with Eqs. (2) and (3):

Table 1
Burn severity classes distribution in Pisan Mountains study area and santo pietro (SP) watershed according to USGS classification of relativized burn ratio (RBR) index (modified).

Severity class	RBR value	% of all burned surface	% of SP watershed surface
Unburned	−0.1 to 0.099	8.6	16.7
Low severity	0.1 to 0.269	19.7	15
Moderate severity	0.27 to 0.659	59	65.7
High severity	0.66 to 1.3	12.6	2.6

Fig. 4. Some examples of burned areas in Pisan Mountains: (a) high burn severity in a pine stand; (b) high burn severity in maquis; (c) low burn severity in maquis; (d) moderate burn severity in a chestnut stand.

$$Q = \begin{cases} 0 & \text{for } P \le I_a \\ \dfrac{(P - I_a)^2}{P - I_a + S} & \text{for } P > I_a \end{cases} \quad (2)$$

where P (mm) is the rainfall depth for the calculation interval, and S (mm) is the potential maximum soil moisture retention calculated as Eq. (3):

$$S = 25.4\left(\frac{1000}{CN} - 10\right) \quad (3)$$

where I_a is the initial abstraction, namely the depth of water retained by the landscape before the runoff starts, by infiltration and rainfall interception by vegetation in millimeters. I_a is generally assumed to be $0.2S$.

The method is based on CN a non-dimensional parameter that accounts for the physical response of a landscape unit to rainfall and ranges from 30 to 100. CN depends upon the soil type and land cover, and the higher CN, the lower the basin losses and, consequently, the larger the runoff. Combining data on soil and land cover, an initial CN value is calculated, namely CNII, valid for average soil moisture conditions. Each CNII corresponds to a CNI (lower) value, to be used for dry soil conditions, and to a CNIII (higher) value for wet conditions (see USDA, 1986, for the complete method and CN value parametrization).

In the current case, the overall average CN for SP watershed in post-fire conditions was obtained by an area-weighted average of the CN of all landscape units falling within the watershed, which was extrapolated from the CN map of Tuscany (Castelli, 2014). Since no significant rain was recorded right after the wildfire and before the simulation date, values for the CN in dry soil conditions (CNI) were used.

Several CN-based methods are available for the modeling of burned landscape conditions. One of these is BAER (burned area emergency response; Napper, 2006), which prescribes increases in CNII of 15, 10, and 5 for areas affected by high, medium, and low-severity fire damage, respectively. Coschignano et al. (2019) applied increases in CN varying from 5 to 20 for growing fire severities. Most of the burned area in SP watershed was characterized by moderate severity. However, aiming to investigate the short-term effect of fire, therefore with the maximum alteration of CN, we applied the procedure of Soulis (2018), who assumed an increase of 25 units in CN for burned areas in a catchment in Greece.

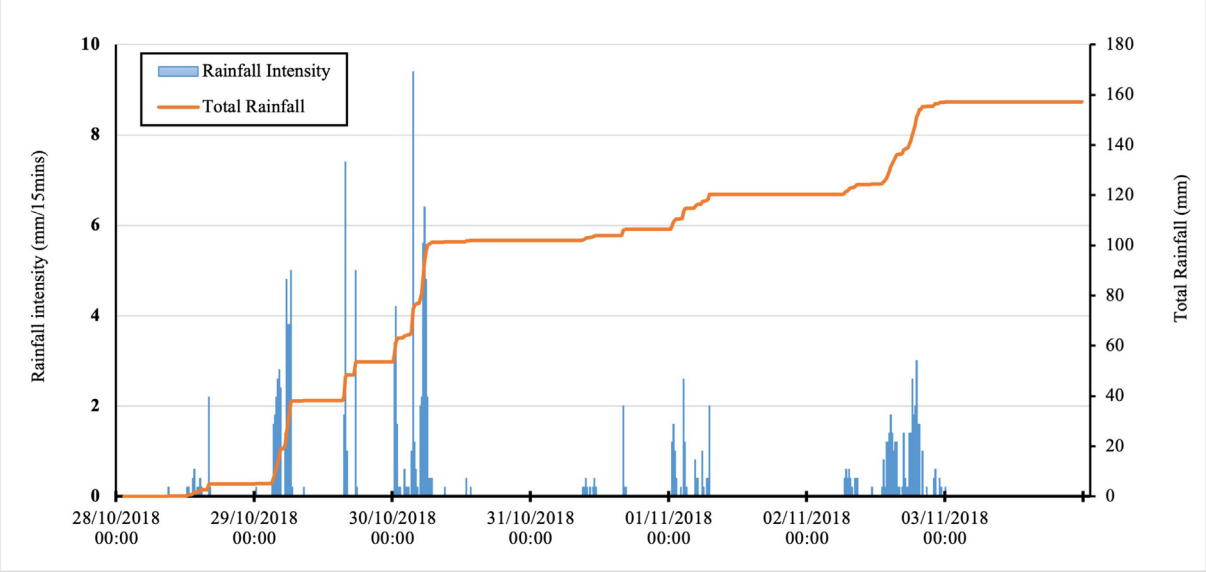

Fig. 5. Rainfall events recorded from October 28 to November 3, 2018, at Monte Serra Station, located at around 2.5 km from SP watershed.

This choice was made because of the similarities between the Soulis study site and our site in terms of environment, vegetation, and fire impact.

The SCS dmensionless unit hydrograph method (USDA, 1986) was used as a rainfall-runoff transformation method ("transform method"). Hence, at each calculation time, the instantaneous runoff generated by the watershed was transformed using a standard hydrograph with a peak time 0.6 times that of the basin concentration time, which meant 27 min for the SP watershed. The overall sub-basin response was calculated as the convolution of all hydrographs.

The HEC-HMS version 4.3 (Hydrologic Engineering Center, 2018) was used for the modeling process, and no baseflow and evapotranspiration process simulations were considered since the model was replicating a peak flow event. The model was not calibrated nor validated since the burned catchments in the area were not gaged at the time of the analysis while validating the model some months after the fire would have led to different catchment conditions due to vegetation regrowth.

2.6. Stream sediment quantification and sampling

A few days after the fire, a large wooden check dam was built to act as a sediment trap at the SP watershed outlet, just before the small town of Calci, to prevent streambed aggradation in the urban area in case of post-fire floods (Fig. 2). No rainfall occurred between the fire and the construction of the structure, while the whole volume of the latter was filled by sediment just after the significant rainfall events described in Section 2.4. Therefore, the sediment volume trapped upstream of the check dam corresponded to the sediment produced by rains that occurred from October 28 to November 3, 2018.

Soon after that time-lapse, a detailed topographic survey was done to measure the location and elevation of a 32-point grid at the surface of the sediment deposit and at the level of the streambed by digging small trenches upstream of the check dam. This allowed the determination of the shape and volume of the deposit (Fig. 3), which was then sampled by metal pipes 12 cm in diameter, driven as deep as possible. The determination of the boundary between the post-fire sediment deposits and the pre-existing streambed was based on the assumption that, due to the relatively high slope of the stream, the original streambed was mainly composed of gravel, which prevented the sampling pipes from being driven deeper. Further discussion on the analysis of the sedimentation dynamics is reported in Section 3.3.

Five deposit cores were taken at five different points and three cores were kept for further analysis (see Fig. 3): one close to the check dam (E), another almost at the opposite extreme of the sedimentation area (B), and the third (A) approximately in between. The core A was the thickest and the one used for the calculation of the volume of the sediment deposit. For each layer identified in this core, the relative deposition volume was determined with a geometric procedure, considering the widening of the trapezoidal section and, at the cut-off length, adjusted accordingly (Fig. 3). The mass of each layer deposited at the check dam site (MD_i) was calculated multiplying the estimated volume by the related bulk density measured in the core (see Section 2.7 for bulk density determination).

The total mass of soil eroded at the catchment scale (ME_i), namely the mass that flowed up to the check dam site (either deposited before or flowed past it with the overflowing water), was calculated from the sediment trap efficiency of the check dam at the time of deposition of the uppermost layer of the core A (STE_i) (Eq. (4)):

$$ME_i = \frac{ME_i}{STE_i} \tag{4}$$

where STE_i was estimated according to Brown (1943), using Eq. (5):

$$STE_i = 1 - \left(\frac{1}{1 - 0.0021 D \frac{C_i}{W}} \right) \tag{5}$$

where C_i (m^3) is the volume capacity upstream of the check dam before the deposition of the uppermost layer of the core A, W is the extension of the watershed upstream of the check dam, and D is a coefficient assumed to be 1 for watersheds with variable and limited runoff.

By analyzing the outputs of the HEC-HMS model (Section 2.5), each sedimentation event (i.e., each layer in the core) was related to a peak flow event during the modeled period, and the sediment concentration was calculated dividing ME_i by the total volume of the flow. Finally, the average post-fire erosion rate was calculated by dividing the total sediment eroded by the area of the SP watershed.

2.7. Soil and sediment analysis

Soil and sediment samples were air-dried and then sieved to 2 mm. The lone fine earth, the smaller than 2-mm fraction, underwent further analysis. Particle size analysis was done according to the hydrometer method. The bulk density of the collected sediment was determined by dividing their weight after oven-drying at

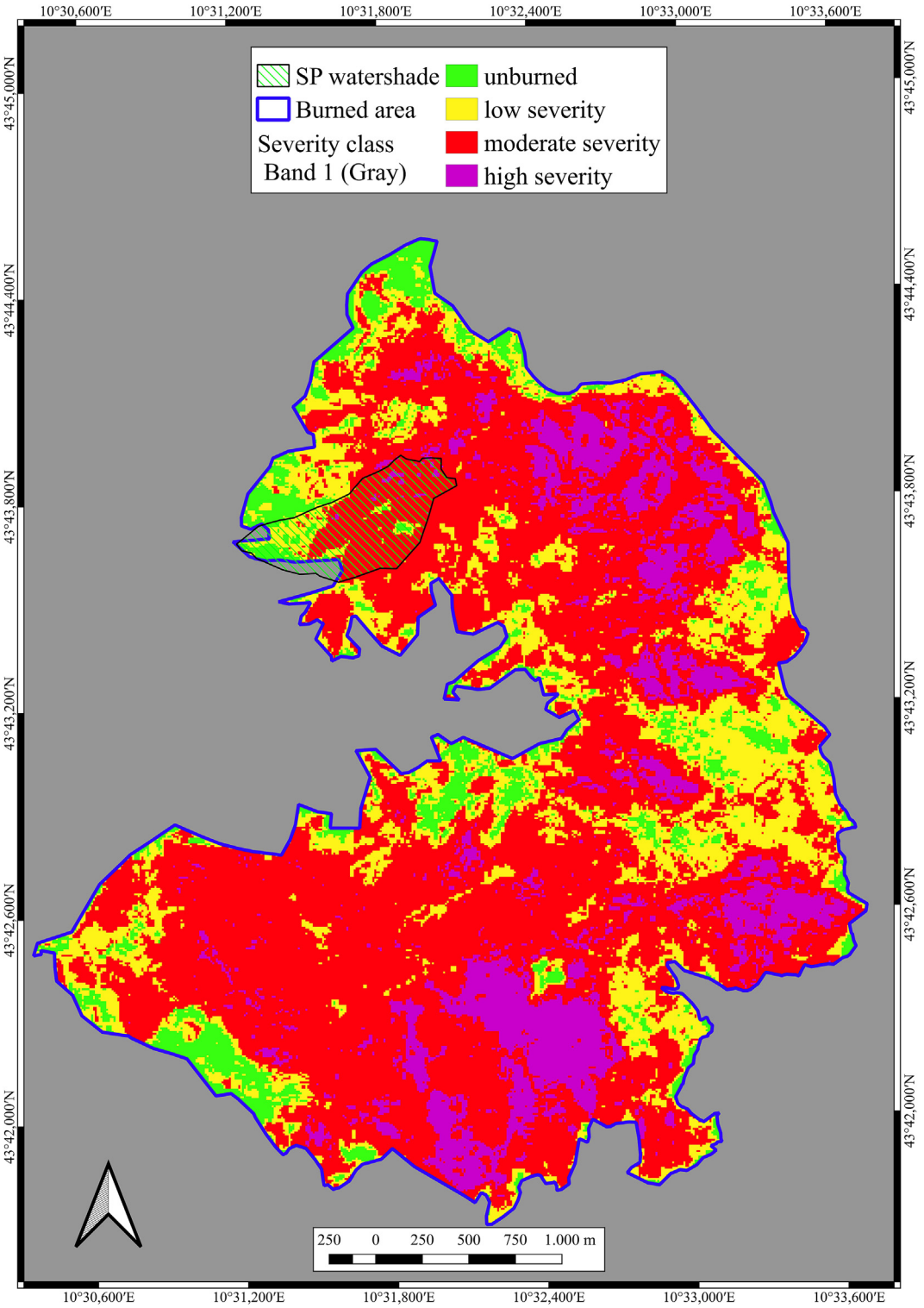

Fig. 6. Fire severity map of study area according to relativized burn ratio index.

105 °C to constant weight by the known volume of the sediment cores. Organic matter was measured as the loss on ignition (LOI) at 480 °C for 8 h.

3. Results

3.1. Burn severity

The burn severity, as registered by remotely sensed data from Sentinel-2 images, is shown in Fig. 6. Most of the SP watershed underwent moderately severe fire, as in the other Pisan Mountains catchments involved in the same wildfire. About 12% of the Pisan Mountains area burned with high severity (Table 1), while just 2% did so in the SP catchment, perhaps because of its proximity to the small town of Calci, where fire suppression efforts were greater than elsewhere. Possibly for the same reason, the unburned surface amounted to over 16% in the SP watershed versus less than 9% in the whole Pisan Mountains area.

Field investigation mostly confirmed the remotely sensed data. In the areas where fire severity was recorded as moderate, most of the litter had been completely burned, leaving a mixture of gray ashes and black char on the soil surface with the charred shrub stems standing. In the areas where fire severity was recorded as high, most of the above-ground biomass, including finer fuels and the shrub layer < 2–3 cm, was consumed and turned into gray or white ash covering the ground, while most of the tree stems were still standing although scorched (Fig. 4). The ash layer apparently was not significantly impacted by wind erosion, and, therefore, the underlying mineral soil as well was unimpacted. Nonetheless, the ash did not stay on the surface for long and was flushed away by the first rains.

3.2. Soil characteristics

In general, the Pisan Mountains' soils were shallow and quite rich in rock fragments. The median thickness was measured as 0.4 m, with a minimum value of 0.1 m and a maximum value of over 1.2 m, the latter just in one plot in the maquis. The median value of stoniness was 16%, with a minimum value of < 1% and a maximum value of over 34%. As a reference, a stone cover of 30% has been shown to imply a consistent reduction of post-fire soil erosion (Prats et al., 2018). Soil texture was quite uniform in the investigated plots and ranged from sandy loam to loam, being composed of half sand and a third of the total by silt on a weight basis.

3.3. Analysis of sediment

The collected cores of sediment retained by the wooden check dam are shown in Fig. 7, while the organic matter content and particle size distribution of the different layers—confidently corresponding to the main episodes of deposition — are listed in Table 2. The maximum thickness of the sediment deposit, 71.5 cm, was found 13 m upstream of the dam. None of the cores contained rock fragments, i.e., larger than 2 mm, or coarse charcoal pieces, which are instead usually abundant in the ash layer covering the burned soils (Mastrolonardo et al., 2017).

The thickest core, core A, showed six distinct layers (A1 to A6, from the surface downwards). The layers A1–A4, overall 40.6 cm thick, were clearly made of post-fire eroded soil, as revealed by the blackish color imposed by the abundant charred materials (Table 2). The layer A4 was much richer in organic matter than all the overlying materials, which was of course brought in by subsequent rainfall. The layers A5–A6, which are the bottom of the deposit (i.e., the first materials that settled), were much different from the upper layers, i.e., lighter, browner, and poorer in organic matter. They differed from each other in organic matter content, the deeper one being poorer. In terms of particle size distribution, there was no clear discontinuity between A1—A4 and A5, A6 sediment layers (Table 2). Nevertheless, with the subsequent rainy events the deposited eroded soil tended to become increasingly coarser from the base upward, i.e., richer in sand and poorer in silt (whereas clay was almost constant and amounting to around 10%).

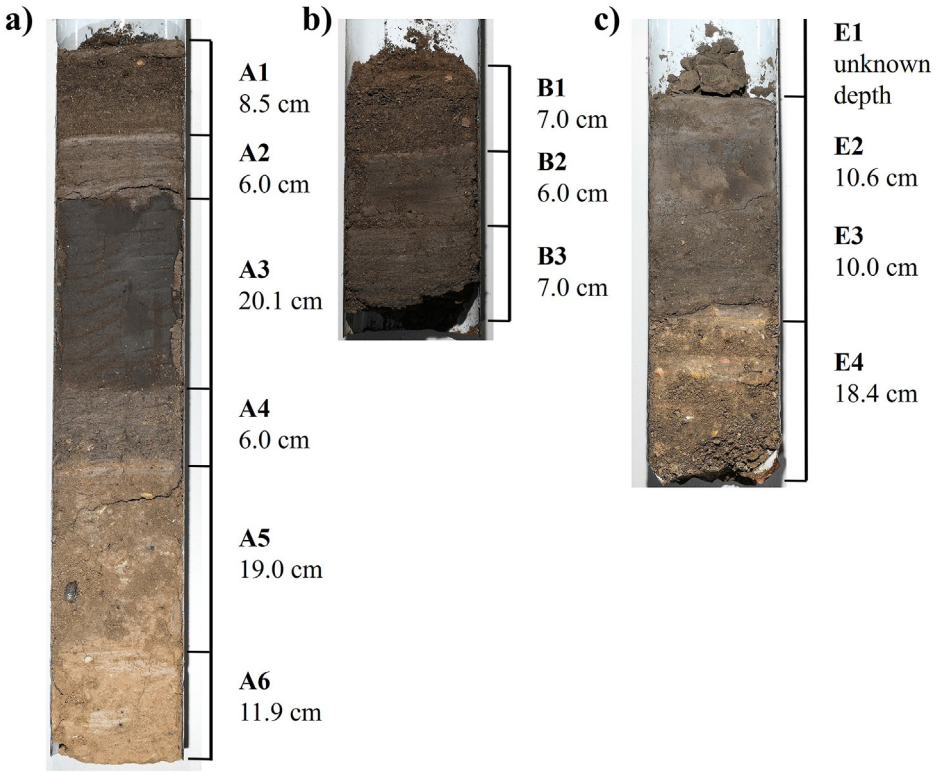

Fig. 7. (a—c) Sediment cores collected upstream of check dam built immediately after wildfire at outlet of Santo Pietro watershed (see Fig. 3 for locations of cores).

The core B was taken several meters upstream of the core A, where the sediment deposit was much thinner. The layers of which were composed approximately of the same material in the uppermost 20 cm of the core A. However, there were some discrepancies between the two cores, such as a much higher organic matter and sand contents in the deepest layer in the core B compared to the corresponding layer in the core A, most probably due to the progressive selective deposition of particles on a weight basis.

The core E comprised four layers, including a brownish layer at the bottom, which looked like the one found at the base of the core A in terms of thickness, organic matter content, and particle size distribution. The blackish material, assumed to be from the burned area, had a more homogeneous appearance than in the other two cores, although still showing three distinct layers. Actually, these latter were similar to each other in terms of both organic matter and particle size distribution. This homogeneity could be explained by the flow turbulence acting in the water close to the check dam, where the core E was from.

3.4. Post-fire rainfall-runoff-erosion

The average CNI calculated for the SP watershed was 71, considering the extent of the burned areas according to the RBR map. Rainfall and runoff time series, together with the hypothesized deposition events within the SP, are shown in Fig. 8, where the main flow events are associated with the six deposition events detected by the analysis of the sediment core A. Coherently, the layer A3 was assigned to the largest flow event.

Table 3 lists the overall results of the analysis, including the values used for sediment trap efficiency calculation. The latter was done considering the same C_i for the events A4 and A3, and for the events A2 and A1, since the two couples of events were very close in time.

By Eq. (1) and the available rainfall data, the Rt of the largest 30-min event monitored was estimated to be one year. The main rainfall-runoff events recorded from October 28 to November 3, 2018, showed a significant correlation with the mass calculated for the deposition layers of the core A, when the six events are considered as a unique population (Fig. 9). However, a second interpretation of the results based on the separation of the A6–A5 events from the A4–A1 ones provided a better regression and additional insight. The sediment concentrations in the runoff events related to the layers A6 and A5 were similar (around 26 g/L) and higher than the ones of the events generating layers A4 to A1. Therefore, the two classes of events could represent two separate groups, both characterized by two linear relations (forced to pass through 0) with $R^2 \approx 1$ (Fig. 9). The values for the layers A4 to A1 were in line with those from other studies dealing with post-fire sedimentation (e.g., García-Comendador et al., 2017; Ryan et al., 2011), which in the current study amounted to 10–14 g/L.

Comparing the precipitation and erosion events at the watershed scale, the soil erosion calculated for the entire SP basin during the rains immediately after the fire was 0.26 mm, corresponding to 7.85 t/ha. This value corresponded to 42% of the watershed average annual potential erosion rate in normal conditions (18.8 t/ha/y) estimated with the USLE method (Regione Toscana, 2017).

4. Discussion

4.1. Sedimentation dynamics

The sequence of sedimentary layers of the core A (Table 2 and Fig. 7) is counter-intuitive, since the bottom layers (A5–A6), which were deposited before layers A1–A4, are poor in charred residues, which are light and, consequently, more prone to be eroded. In this framework, the proposed hypothesis posits that the first rainfall events and the subsequent peak flows initially transported fire-unaffected sediment, located near or within the stream, to the sedimentation site. This situation has also been documented by Esposito et al. (2017) in a burned watershed in Southern Italy, while Nunes et al. (2020) observed very long times for post-fire relocation of eroded soil in a catchment in the north-western Iberian Peninsula. According to the aforementioned hypothesis, the burned soil eroded from the SP slopes reached the channel and was consequently trapped by the check dam after some hours from the beginning of the rain. This would explain the virtual lack of organic material in the layer A6. The layer A5 was richer in organic matter than the underlying one, revealing that some of the burned sediment intermixed with the previously eroded material had reached the dam in the second deposition event.

The increasing coarseness of texture from the bottom layer A6 to the layer A1 could be a consequence of progressive depletion in silt-sized particles of the residual soil of the watershed. In this regard, Shakesby et al. (2003), studying two small catchments in Australia on sandstone bedrock affected by fires of different severity, found that the sediment transported downstream was richer in organic matter and fines (< 63 μm particles) than those deposited on the slopes, possibly prone to further erosion. The layer A3, the thickest one (20 cm), was rather homogenous and apparently put in place by a single runoff event, fast and uninterrupted. This is confirmed by the HEC-HMS model results (Fig. 8), which show that layer A3 was generated by the largest runoff event, although it comprised two flow peaks induced by a bimodal rainfall pattern. On the contrary, the two overlying layers, A2 and A1, were finely stratified,

Table 2
Depth, thickness, bulk density (BD), organic matter content, and particle size distribution (on a weight basis) of layers in investigated sediment cores from Santo Pietro (SP) watershed.

Core	Layer	Depth	Thickness	BD (g/cm)	Organic matter (%)	Sand (%)	Silt (%)	Clay (%)
A	A1	0–8.5 cm	8.5 cm	0.53	23.1	64.7	25.5	9.8
	A2	8.5–14.5 cm	6.0 cm	0.49	21.3	53.3	37.2	9.5
	A3	14.5–34.6 cm	20.1 cm	0.66	19.4	41.0	50.8	8.1
	A4	34.6–40.6 cm	6.0 cm	0.56	32.1	46.1	44.1	9.8
	A5	40.6–59.6 cm	19.0 cm	0.93	9.1	45.2	44.1	10.7
	A6	59.6–71.5 cm	11.9 cm	1.02	3.9	32.2	54.7	13.1
B	B1	0–6 cm	6 cm	nd	25.6	70.1	23.3	6.6
	B2	6–13 cm	7 cm	nd	21.7	38.6	55.0	6.4
	B3	13–20 cm	7 cm	nd	26.4	50.2	40.5	9.4
E	E1	0–3 cm	3 cm	nd	16.5	41.0	49.1	9.9
	E2	3–13.6 cm	10.6 cm	nd	16.4	32.2	57.7	10.1
	E3	13.6–23.6 cm	10.0	nd	19.8	47.7	42.7	9.6
	E4	23.6–42 cm	18.4	nd	10.4	46.5	41.0	12.5

Note: nd, not determined.

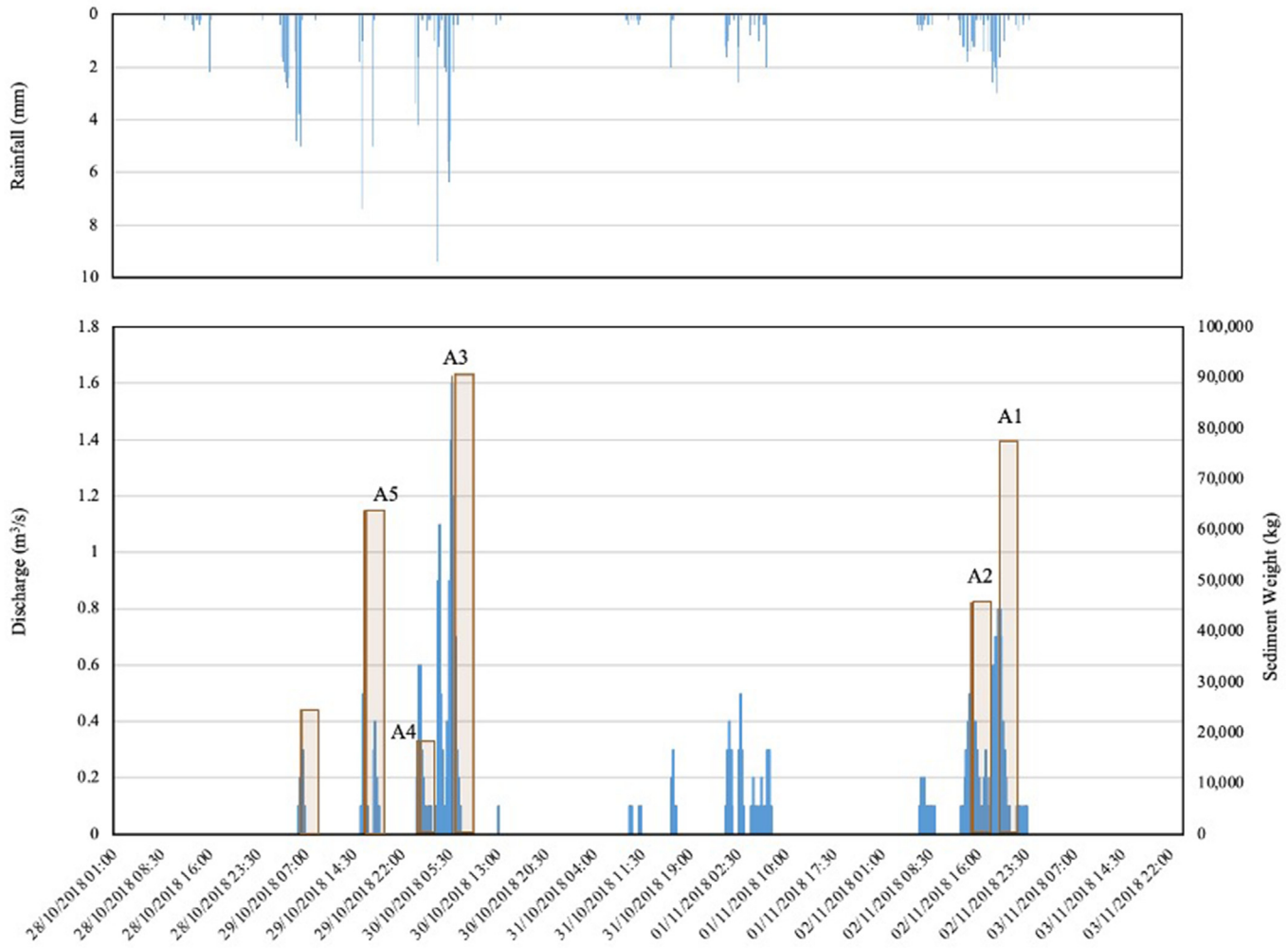

Fig. 8. Rainfall and simulated runoff time series and weight of sediment transported by flow events (brown bars) at outlet of Santo Pietro watershed.

suggesting a discontinuous deposition. Since the outlet where the erosion was inferred is located after a relatively large, unburned area, it is plausible that this latter acted as a redeposition area for part of the material eroded upstream, which had not yet reached the dam and was, therefore, not detected in the current study.

4.2. Erosion rate and sediment yield

The first two rainfall events analyzed for the SP watershed — those that most plausibly resulted in layers A6 and A5—transported an overall higher concentration of sediment than the subsequent rainfall events, which can be explained by one or both the following reasons: i) the first two floods have remobilized the carbon-poor material accumulated near the river bed or already in it (as explained in Section 3.3); and/or ii) the initial sediment yield has been fed by the operations for building some erosion control structures, including the check dams on the SP stream, as also found elsewhere by other studies (e.g., Malvar et al., 2017). The second hypothesis is consistent with the lower presence of organic matter in the layers A6–A5 compared to the overlying layers. Although the model used was not validated, leading to high relative uncertainty in the estimation of sediment concentrations, the differences between the first two events and the following four events are consistent and can be considered representative of the overall sediment mobilization dynamics at the catchment scale.

The estimated erosion rate in the SP watershed, 7.85 t/ha, is comparable to that found in other studies, such as the one by Kampf et al. (2016). These authors measured an average loss of 5.9 t/ha after some summer storms, of intensities comparable with those considered in our study, and observed a couple of months after a fire that affected a forest stand predominantly composed of Ponderosa pine on stony, sandy loam soils in Colorado, U.S. On the other hand, the results we found are quite lower than those from other studies. For instance, Esposito et al. (2017) measured sediment yield ranging from 19.8 to 33.1 t/ha in 11 ha watershed in Southern Italy on fresh volcanic deposits resulting from an intense rainstorm that happened one month after a wildfire. Similarly, Robichaud et al. (2013) reported soil losses of 18.6–24.4 t/ha after two high-intensity rainstorms in a previously burned 4.6 ha watershed in Colorado, U.S. These studies, however, dealt with slightly higher-intensity rainfalls than in the current study.

On a longer term, again at the catchment scale, Mayor et al. (2007) measured 35 mm and 4.6 t/ha as the total volume of runoff and sediment yield for 7 years (from 1999 to 2005) after a wildfire near Alicante, Spain. In a 72 km^2 catchment in southern Italy, Grangeon et al. (2021) checked over a 7 month period including 21 flood events (from November 2010 to May 2011), finding that the mean sediment yield had increased by 5% and up to a maximum of 37% because of the fire, ranging from 2.0 to 2.7 t/ha/y depending on the burned area. Simulating the fire sediment yield

Table 3
Values of peak discharge, flow, sediment concentration, volume, and mass (MD_i) at check dam site, volume capacity upstream check dam (C_i), sediment trap efficiency (STE_i), and sediment eroded at catchment scale (ME_i) for Santo Pietro (SP) watershed.

Layer	Peak discharge (m^3/s)	Flow event volume (m^3)	Sediment volume at check dam site (m^3)	MD_i (t)	C_i (m^3)	STE_i	ME_i (t)	Sediment concentration (g/L–kg/m^3)
A6	0.3	900	10.22	10.43	142.60	0.42	24.64	27
A5	0.6	2,430	27.86	25.91	132.38	0.41	63.94	26
A4	0.6	1,800	11.35	6.36	104.52	0.35	18.17	10
A3	1.6	8,910	47.94	31.64	104.50	0.35	90.46	10
A2	0.5	3,510	17.57	8.61	45.21	0.19	45.61	13
A1	0.8	5,400	27.65	14.65	45.21	0.19	77.61	14

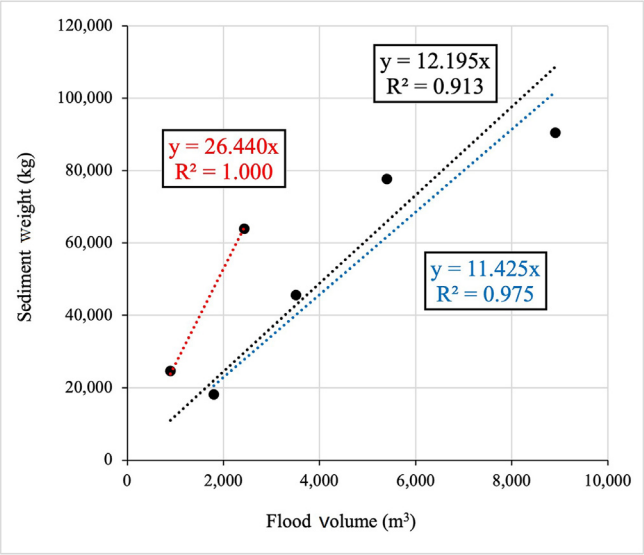

Fig. 9. Correlation of flow and sedimentation events at outlet of Santo Pietro watershed. Black trendline: A6–A1 regression; red trendline: A6–A5 regression; and blue trendline: A4–A1 regression.

after a high-severity fire and post-fire logging activities using the SWAT model in two sub-basins approximately 72 km^2 wide in southern Italy, De Girolamo et al. (2022) found values as high as 26–54 t/ha/y (baseline values of 9.5–9.7 t/ha/y), the variability strongly depending on the relative extent of the fire affected area. However, a comparison of our data with those from longer-term studies could be somewhat improper as we took into account just the first rains after the fire. Nonetheless, in the Mediterranean basin, the period of high susceptibility to erosion of burned soils is typically short as the maximum fire potential is during the dry summer (July–August), which is followed by a rainy autumn (Granged et al., 2011; Lucas-Borja et al., 2019; Shakesby, 2011).

The fire-induced impact on soil is the combination/interaction of various factors, in particular fire severity and extent, terrain slope, rainfall intensity, and soil infiltrability (the "fire nexus" *sensu* Neary, 2019). The Pisan Mountains have steep slopes characterized by high erosion rates and studied wildfire, whose severity was moderate to high, theoretically had to result in dramatic soil erosion even with relatively modest rainfall events. Nonetheless, this did not happen, at least in the SP watershed. Often, post-fire erosion rates in the Mediterranean area have been reported to be relatively modest, ranging from 0.016 to 13.1 t/ha/y (Shakesby, 2011), mainly because of the shallow, skeleton-rich soils that i) provide a limited amount of fines and ii) are endowed with a stony pavement, which protects the underlying soil from erosion (Shakesby, 2011). These features encourage water infiltration and limit the formation of a continuous fire-induced water-repellency layer (Urbanek & Shakesby, 2009; Wu et al., 2021). Indeed, this scenario holds true for our study area, where also previous fire events have already depleted a significant portion of the highly erodible finest fraction of soil.

A relatively moderate soil loss, however, does not necessarily correspond to an equally moderate negative impact on the ecosystem. In fact, most of the organic matter and nutrients are concentrated near the surface, and thus topsoil erosion negatively affects both soil fertility and water quality (Basso et al., 2019), especially in an already degraded situation such as the one currently studied (Shakesby et al., 2015; Verheijen et al., 2009). Here as elsewhere in the Mediterranean region, the application of soil and water bioengineering solutions, such as cover and barrier treatments, can hinder the progression of erosion in a sustainable way (Florineth, 2012; Girona-García et al., 2021; Preti et al., 2022). Particularly in severely burned areas, economically viable and effective measures are strongly requested to stabilize the slopes (Girona-García et al., 2021; Zaimes et al., 2020), as well as to drain and control runoff (Florineth, 2012).

5. Conclusions

The current paper inspects the short-term hydrological impacts at the watershed scale of a fire of moderate to high severity that involved the Pisan Mountains in central Italy. Given the extensive nature of the fire, the significant loss of vegetation cover, and the steep slopes, it is hypothesized that a notable increase in post-fire soil erosion would occur. This watershed-scale investigation, done using an HEC-HMS model, and the sediment yields, inferred by sediment cores taken upstream of the last check dam, allowed the estimation of the eroded soil through the dynamic calculation of sediment trap efficiency. This amounted to 7.85 t/ha, which is unexpectedly moderate considering the high average annual potential erosion rate of the watershed. Such a relatively low fire-induced soil loss can be the result of the shallowness of soils and the abundance of outcrops and emerging rock fragments. The analysis of sediment cores also suggested that materials already present in stream could have been moved up to the outlet of the study area by first rainfall showers, while the burned sediment was delivered later.

Comparing these findings with those from other studies in the Mediterranean region highlights the considerable variability in post-fire hydrological response, even in comparable conditions of fire severity, wildfire scale, slope, and post-fire rainfall. These results emphasize the importance of incorporating multiple analytical studies addressing the various specific and diverse conditions for more accurate predictions of hydrological and erosive risks. Such an approach would be crucial for effective management in fire-affected Mediterranean environments and could be reproduced in those cases where civil works aiming at retaining sediment should be implemented but the available data are scarce. The results from these investigations, if well integrated with watershed planning, are useful in indicating how quickly check dams built to reduce flood risk would fill, and if complementary infrastructure is needed.

Future investigation in this and similar environments should further investigate the empirical analysis of erosion patterns, as well as targeting hydrological and sedimentological post-fire modeling, assessing ecological impacts of wildfires, and monitoring post-fire recover dynamics, especially from a hydrological point of view, including groundwater.

Data accessibility statement

Data will be made available upon reasonable request.

Author contributions

Giovanni Mastrolonardo: Conceptualization, Methodology, Formal Analysis, Investigation, Resources, Data curation, Writing–original draft, Writing–review & editing. **Giulio Castelli**: Conceptualization, Methodology, Formal Analysis, Investigation, Data curation, Writing–original draft, Writing–review & editing, Visualization, Supervision. **Giacomo Certini**: Conceptualization, Formal Analysis, Writing–review & editing. **Melanie Maxwald**: Methodology, Investigation, Data curation, Writing–review & editing. **Paolo Trucchi**: Methodology, Investigation, Data curation, Formal Analysis, Writing–review & editing. **Cristiano Foderi:** Investigation, Data curation, Writing–review & editing, Visualization. **Alessandro Errico:** Conceptualization, Methodology, Formal Analysis, Investigation, Data curation, Writing–review & editing. **Elena Marra:** Formal Analysis, Investigation, Resources, Data curation, Writing–review & editing. **Federico Preti:** Conceptualization, Methodology, Formal Analysis, Investigation, Data curation, Writing–review & editing, Supervision, Funding acquisition, Project administration.

Declaration of competing interest

The authors declare that they have no known competing financial interests or personal relationships that could have appeared to influence the work reported in this paper.

Acknowledgements

The authors are grateful to Lorenzo Gardin for the information supporting the erosion analysis, and Samantha Benucci and Silva Calvani for their work during the soil sampling in the Pisan Mountains. The authors also are grateful to all anonymous reviewers who provided useful comments and insight for improving the paper. The authors finally thank Consorzio di Bonifica Basso Valdarno, Italy, for funding under the agreement for research activities “Monitoraggio dissesto post incendio”.

References

Abraham, J., Dowling, K., & Florentine, S. (2017). Risk of post-fire metal mobilization into surface water resources: A review. *Science of the Total Environment, 599–600*, 1740–1755.

Basso, M., Vieira, D. C. S., Ramos, T. B., & Mateus, M. (2020). Assessing the adequacy of SWAT model to simulate postfire effects on the watershed hydrological regime and water quality. *Land Degradation & Development, 31*, 619–631.

Brown, C. B. (1943). Discussion of sedimentation in reservoirs. In J. Witzig (Ed.), *Proceedings of the American Society of civil Engineers, 69* (pp. 1493–1500).

Castelli, F. (2014). Implementazione di modello idrologico distribuito per il territorio toscano - Regione Toscana. Retrieved from https://www.regione.toscana.it/-/implementazione-di-modello-idrologico-distribuito-per-il-territorio-toscano.

Coschignano, G., Nicolaci, A., Ferrari, E., Cruscomagno, F., & Iovino, F. (2019). Evaluation of hydrological and erosive effects at the basin scale in relation to the severity of forest fires. *iForest, 12*, 427–434.

De Girolamo, A. M., Cerdan, O., Grangeon, T., Ricci, G. F., Vandromme, R., & Lo Porto, A. (2022). Modelling effects of forest fire and post-fire management in a catchment prone to erosion: Impacts on sediment yield. *Catena, 212*, 106080.

Ebel, B. A. (2020). Temporal evolution of measured and simulated infiltration following wildfire in the Colorado Front Range, USA: Shifting thresholds of runoff generation and hydrologic hazards. *Journal of Hydrology, 585*, 124765.

Esposito, G., Matano, F., Molisso, F., Ruoppolo, G., Di Benedetto, A., & Sacchi, M. (2017). Post-fire erosion response in a watershed mantled by volcaniclastic deposits, Sarno Mountains, Southern Italy. *Catena, 152*, 227–241.

Fernández, C., Vega, J. A., & Fontúrbel, T. (2016). Reducing post-fire soil erosion from the air: Performance of heli-mulching in a mountainous area on the coast of NW Spain. *Catena, 147*, 489–495.

Florineth, F. (2012). *Pflanzen statt Beton*. Berlin: Patzer Verlag. *(In German)*

Franceschelli, M., Leoni, L., Memmi, I., & Puxeddu, M. (1986). Regional distribution of Al-silicates and metamorphic zonation in the low-grade Verrucano metasediments from the Northern Apennines, Italy. *Journal of Metamorphic Geology, 4*, 309–321.

García-Comendador, J., Fortesa, J., Calsamiglia, A., Calvo-Cases, A., & Estrany, J. (2017). Post-fire hydrological response and suspended sediment transport of a terraced Mediterranean catchment. *Earth Surface Processes and Landforms, 42*, 2254–2265.

Giorgetti, G., Goffé, B., Memmi, I., & Nieto, F. (1998). Metamorphic evolution of Verrucano metasediments in northern Apennines: New petrological constraints. *European Journal of Mineralogy, 10*, 1295–1308.

Girona-García, A., Vieira, D. C. S., Silva, J., Fernández, C., Robichaud, P. R., & Keizer, J. J. (2021). Effectiveness of post-fire soil erosion mitigation treatments: A systematic review and meta-analysis. *Earth-Science Reviews, 217*, 103611.

Granath, G., Moore, P. A., Lukenbach, M. C., & Waddington, J. M. (2016). Mitigating wildfire carbon loss in managed northern peatlands through restoration. *Scientific Reports, 6*, 28498.

Granged, A. J. P., Zavala, L. M., Jordán, A., & Bárcenas-Moreno, G. (2011). Post-fire evolution of soil properties and vegetation cover in a mediterranean heathland after experimental burning: A 3-year study. *Geoderma, 164*, 85–94.

Grangeon, T., Vandromme, R., Cerdan, O., De Girolamo, A. M., & Lo Porto, A. (2021). Modelling forest fire and firebreak scenarios in a Mediterranean mountainous catchment: Impacts on sediment loads. *Journal of Environmental Management, 289*, 112497.

Greenbaum, N., Wittenberg, L., Malkinson, D., & Inbar, M. (2021). Hydrological and sedimentological changes following the 2010-forest fire in the Nahal Oren Basin, Mt. Carmel Israel–a comparison to pre-fire natural rates. *Catena, 196*, 104891.

Hydrologic Engineering Center. (2018). *HEC-HMS User's Manual version 4.3*.

Kampf, S. K., Brogan, D. J., Schmeer, S., MacDonald, L. H., & Nelson, P. A. (2016). How do geomorphic effects of rainfall vary with storm type and spatial scale in a post-fire landscape? *Geomorphology, 273*, 39–51.

Kampf, S. K., Gannon, B. M., Wilson, C., Saavedra, F., Miller, M. E., Heldmyer, A., Livneh, B., Nelson, P., & MacDonald, L. (2020). PEMIP: Post-fire erosion model inter-comparison project. *Journal of Environmental Management, 268*, 110704.

Keeley, J. E. (2009). Fire intensity, fire severity and burn severity: A brief review and suggested usage. *International Journal of Wildland Fire, 18*, 116–126.

Köthe, H. (2003). Existing sediment management guidelines: An overview. *Journal of Soils and Sediments, 3*, 139–143.

Larsen, I. J., MacDonald, L. H., Brown, E., Rough, D., Welsh, M. J., Pietraszek, J. H., Libohova, Z., de Dios Benavides-Solorio, J., & Schaffrath, K. (2009). Causes of post-fire runoff and erosion: Water repellency, cover, or soil sealing? *Soil Science Society of America Journal, 73*, 1393–1407.

Lucas-Borja, M. E., González-Romero, J., Plaza-Álvarez, P. A., Sagra, J., Gómez, M. E., Moya, D., Cerdà, A., & de las Heras, J. (2019). The impact of straw mulching and salvage logging on post-fire runoff and soil erosion generation under Mediterranean climate conditions. *Science of the Total Environment, 654*, 441–451.

Malvar, M. C., Silva, F. C., Prats, S. A., Vieira, D. C. S., Coelho, C. O. A., & Keizer, J. J. (2017). Short-term effects of post-fire salvage logging on runoff and soil erosion. *Forest Ecology and Management, 400*, 555–567.

Mastrolonardo, G., Hudspith, V. A., Francioso, O., Rumpel, C., Montecchio, D., Doerr, S. H., & Certini, G. (2017). Size fractionation as a tool for separating charcoal of different fuel source and recalcitrance in the wildfire ash layer. *Science of the Total Environment, 595*, 461–471.

Mayor, Á. G., Bautista, S., & Bellot, J. (2011). Scale-dependent variation in runoff and sediment yield in a semiarid Mediterranean catchment. *Journal of Hydrology, 397*, 128–135.

Mayor, Á. G., Bautista, S., Llovet, J., & Bellot, J. (2007). Post-fire hydrological and erosional responses of a Mediterranean landscape: Seven years of catchment-scale dynamics. *Catena, 71*, 68–75.

Moody, J. A., & Martin, D. A. (2009). Synthesis of sediment yields after wildland fire in different rainfall regimes in the western United States. *International Journal of Wildland Fire, 18*, 96–115.

Mori, L., Nigro, M., Barneschi, I., Doveri, M., Menichini, M., & Giannecchini, R. (2023). Soils hydraulic conductivity tests in slopes affected by fire: An example on Pisani Mountains (Tuscany, Italy). *Rendiconti Online della Società Geologica Italiani, 61*, 88–93.

Napper, C. (2006). *Burned area emergency response treatments catalog*. San Dimas, CA: United States Department of Agriculture, Forest Service, National Technology & Development Program, Watershed, Soil, Air Management.

Neary, D. G. (2019). Forest soil disturbance: Implications of factors contributing to the wildland fire Nexus. *Soil Science Society of America Journal, 83*, S228–S243.

Nunes, J. P., Bernard-Jannin, L., Rodríguez-Blanco, M. L., Boulet, A. K., Santos, J. M., & Keizer, J. J. (2020). Impacts of wildfire and post-fire land management on

hydrological and sediment processes in a humid Mediterranean headwater catchment. *Hydrological Processes, 34*, 5210–5228.
Panagos, P., Borrelli, P., Poesen, J., Ballabio, C., Lugato, E., Meusburger, K., Montanarella, L., & Alewell, C. (2015). The new assessment of soil loss by water erosion in Europe. *Environmental Science & Policy, 54*, 438–447.
Parks, S. A., Dillon, G. K., & Miller, C. (2014). A new metric for quantifying burn severity: The relativized burn ratio. *Remote Sensing, 6*, 1827–1844.
Parson, A., Robichaud, P. R., Lewis, S. A., Napper, C., & Clark, J. T. (2010). *Field guide for mapping post-fire soil burn severity. General Technical Report RMRS-GTR-243*. Fort Collins, CO: U.S. Department of Agriculture, Forest Service, Rocky Mountain Research Station.
Parsons, A. J., Brazier, R. E., Wainwright, J., & Powell, D. M. (2006). Scale relationships in hillslope runoff and erosion. *Earth Surface Processes and Landforms, 31*, 1384–1393.
Pausas, J. G., Llovet, J., Rodrigo, A., & Vallejo, R. (2008). Are wildfires a disaster in the Mediterranean basin? A review. *International Journal of Wildland Fire, 17*, 713–723.
Peel, M. C., Finlayson, B. L., & McMahon, T. A. (2007). Updated world map of the Köppen-Geiger climate classification. *Hydrology and Earth System Sciences, 11*, 1633–1644.
Poesen, J. W. A., & Hooke, J. M. (1997). Erosion, flooding and channel management in Mediterranean environments of southern Europe. *Progress in Physical Geography: Earth and Environment, 21*, 157–199.
Powlson, D. S., Whitmore, A. P., & Goulding, K. W. T. (2011). Soil carbon sequestration to mitigate climate change: A critical re-examination to identify the true and the false. *European Journal of Soil Science, 62*, 42–55.
Prats, S. A., Abrantes, J. R. C. B., Coelho, C., Keizer, J. J., & de Lima, J. L. M. P. (2018). Comparing topsoil charcoal, ash, and stone cover effects on the postfire hydrologic and erosive response under laboratory conditions. *Land Degradation & Development, 29*, 2102–2111.
Preti, F. (2013). Forest protection and protection forest: Tree root degradation over hydrological shallow landslides triggering. *Ecological Engineering, 61*, 633–645.
Preti, F., Capobianco, V., & Sangalli, P. (2022). Soil and water bioengineering (SWB) is and has always been a nature-based solution (NBS): A reasoned comparison of terms and definitions. *Ecological Engineering, 181*, 106687.
Preti, F., Forzieri, G., & Chirico, G. B. (2011). Forest cover influence on regional flood frequency assessment in Mediterranean catchments. *Hydrology and Earth System Sciences, 15*, 3077–3090.
Regione Toscana. (2017). Database pedologico. Retrieved from https://www502.regione.toscana.it/geoscopio/pedologia.html.
Robichaud, P. R., Wagenbrenner, J. W., Lewis, S. A., Ashmun, L. E., Brown, R. E., & Wohlgemuth, P. M. (2013). Post-fire mulching for runoff and erosion mitigation Part II: Effectiveness in reducing runoff and sediment yields from small catchments. *Catena, 105*, 93–111.
Robichaud, P. R., Wagenbrenner, J. W., Pierson, F. B., Spaeth, K. E., Ashmun, L. E., & Moffet, C. A. (2016). Infiltration and interrill erosion rates after a wildfire in western Montana, USA. *Catena, 142*, 77–88.
Robinne, F., Hallema, D. W., Bladon, K. D., Flannigan, M. D., Boisramé, G., Bréthaut, C. M., Doerr, S. H., Di Baldassarre, G., Gallagher, L., Hohner, A. K., Khan, S. J., Kinoshita, A. M., Martin, D., Mordecai, R., Nunes, J. P., Nyman, P., Santín, C., Sheridan, G., Stoof, C. R., … Wei, Y. (2021). Scientists' warning on extreme wildfire risks to water supply. *Hydrological Processes, 35*, e14086.
Rulli, M. C., Bozzi, S., Spada, M., Bocchiola, D., & Rosso, R. (2006). Rainfall simulations on a fire disturbed mediterranean area. *Journal of Hydrology, 327*, 323–338.
Rulli, M. C., & Rosso, R. (2007). Hydrologic response of upland catchments to wildfires. *Advances in Water Resources, 30*, 2072–2086.
Ryan, S. E., Dwire, K. A., & Dixon, M. K. (2011). Impacts of wildfire on runoff and sediment loads at Little Granite Creek, western Wyoming. *Geomorphology, 129*, 113–130.
Scharffenberg, B., Bartles, M., Brauer, T., Fleming, M., & Karlovits, G. (2018). *Hydrologic modeling system HEC-HMS user's manual*. Davis, CA: U.S. Army Corps of Engineers, Institute for Water Resources, Hydrologic Engineering Center (CEIWR-HEC).
Shakesby, R. A. (2011). Post-wildfire soil erosion in the Mediterranean: Review and future research directions. *Earth-Science Reviews, 105*, 71–100.
Shakesby, R. A., Bento, C. P. M., Ferreira, C. S. S., Ferreira, A. J. D., Stoof, C. R., Urbanek, E., & Walsh, R. P. D. (2015). Impacts of prescribed fire on soil loss and soil quality: An assessment based on an experimentally-burned catchment in central Portugal. *Catena, 128*, 278–293.
Shakesby, R. A., Chafer, C. J., Doerr, S. H., Blake, W. H., Wallbrink, P., Humphreys, G. S., & Harrington, B. A. (2003). Fire severity, water repellency characteristics and hydrogeomorphological changes following the Christmas 2001 Sydney forest fires. *Australian Geographer, 34*, 147–175.
Shakesby, R. A., & Doerr, S. H. (2006). Wildfire as a hydrological and geomorphological agent. *Earth-Science Reviews, 74*, 269–307.
Soil Survey Staff. (2003). *Keys to soil taxonomy* (9th ed.). Washington, DC: United States Department of Agriculture, Natural Resources Conservation Service.
Soulis, K. X. (2018). Estimation of SCS curve number variation following forest fires. *Hydrological Sciences Journal, 63*, 1332–1346.
Stavi, I. (2019). Wildfires in grasslands and shrublands: A review of impacts on vegetation, soil, hydrology, and geomorphology. *Water, 11*, 1042.
Thomas, G., Rosalie, V., Olivier, C., & Antonio, L. P. (2021). Modelling forest fire and firebreak scenarios in a mediterranean mountainous catchment: Impacts on sediment loads. *Journal of Environmental Management, 289*, 112497.
Thompson, A. L., Gantzer, C. J., & Anderson, S. H. (1991). Topsoil depth, fertility, water management, and weather influences on yield. *Soil Science Society of America Journal, 55*, 1085–1091.
Urbanek, E., & Shakesby, R. A. (2009). Impact of stone content on water movement in water-repellent sand. *European Journal of Soil Science, 60*, 412–419.
USDA. (1986). *Urban hydrology for small watersheds. Technical Release 55 (TR-55) (Second ed.)*. USA: Natural Resources Conservation Service, Conservation Engineering Division.
Vega, S. P., Williams, C. J., Brooks, E. S., Pierson, F. B., Strand, E. K., Robichaud, P. R., Brown, R. E., Seyfried, M. S., Lohse, K. A., Glossner, K., Pierce, J. L., & Roehner, C. (2020). Interaction of wind and cold-season hydrologic processes on erosion from complex topography following wildfire in sagebrush steppe. *Earth Surface Processes and Landforms, 45*, 841–861.
Verheijen, F. G. A., Jones, R. J. A., Rickson, R. J., & Smith, C. J. (2009). Tolerable versus actual soil erosion rates in Europe. *Earth-Science Reviews, 94*, 23–38.
Vieira, D. C. S., Borrelli, P., Jahanianfard, D., Benali, A., Scarpa, S., & Panagos, P. (2023). Wildfires in Europe: Burned soils require attention. *Environmental Research, 217*, 114936.
Wagenbrenner, J. W., & Robichaud, P. R. (2014). Post-fire bedload sediment delivery across spatial scales in the interior western United States. *Earth Surface Processes and Landforms, 39*, 865–876.
Weninger, T., Filipović, V., Mešić, M., Clothier, B., & Filipović, L. (2019). Estimating the extent of fire induced soil water repellency in Mediterranean environment. *Geoderma, 338*, 187–196.
Wilson, C., Kampf, S. K., Ryan, S., Covino, T., MacDonald, L. H., & Gleason, H. (2021). Connectivity of post-fire runoff and sediment from nested hillslopes and watersheds. *Hydrological Processes, 35*, e13975.
Wischmeier, W. H., & Smith, D. D. (1978). Predicting rainfall erosion losses. A guide to conservation planning. In *The USDA Agricultural Handbook No. 537, Maryland, US*. https://www.researchgate.net/profile/Heriansyah-Putra-2/post/Which-formula-is-correct/attachment/59d64d4e79197b80779a6e2c/AS%3A487650378424321%401493276318482/download/USLE.pdf.
Wu, J., Baartman, J. E. M., & Nunes, J. P. (2021). Comparing the impacts of wildfire and meteorological variability on hydrological and erosion responses in a Mediterranean catchment. *Land Degradation & Development, 32*, 640–653.
Zaimes, G. N., Kasapidis, I., Gkiatas, G., Pagonis, G., Savvopoulou, A., & Iakovoglou, V. (2020). Targeted placement of soil erosion prevention works after wildfires. *IOP Conference Series: Earth and Environmental Science, 612*, 012050.
Zema, D. A. (2021). Postfire management impacts on soil hydrology. *Current Opinion in Environmental Science & Health, 21*, 100252.